

Two-Photon Fluorescent Probes for Long-Term Imaging of Calcium Waves in Live Tissue

Hwan Myung Kim,^[a] Bo Ra Kim,^[a] Myoung Jin An,^[a] Jin Hee Hong,^[b]
Kyoung J. Lee,^[b] and Bong Rae Cho*^[a]

Abstract: 2-Acetyl-6-(dimethylamino)-naphthalene-derived two-photon fluorescent Ca^{2+} probes (ACa1–ACa3) are reported. They can be excited by a 780 nm laser beam, show 23–50-fold enhancement in one- and two-photon excited fluorescence in response to Ca^{2+} , emit fourfold stronger two-photon excited fluorescence than

Oregon Green 488 BAPTA-1 upon complexation with Ca^{2+} , and can selectively detect intracellular free Ca^{2+} ions in live cells and living tissues with

minimum interference from other metal ions and membrane-bound probes. Moreover, these probes are capable of monitoring calcium waves at a depth of 120–170 μm in live tissues for 1100–4000 s using two-photon microscopy with no artifacts of photobleaching.

Keywords: calcium • fluorescent probes • imaging agents • live tissue • two-photon microscopy

Introduction


Calcium is a ubiquitous intracellular messenger; it is an essential regulator of many cellular processes including fertilization, cell death, sensory transduction, muscle contraction, motility, exocytosis, and fluid secretion.^[1,2] Calcium triggers exocytosis within microseconds, drives the gene transcription and proliferation in minutes to hours, and the concentration varies from 100 nM at rest to 1 μM upon activation.^[1,2] Defective Ca^{2+} signaling is a feature of diverse diseases including hypertension and immunodeficiencies. To understand these functions, fluorescence imaging with one-photon (OP) fluorescent probes has most often been used.^[3,4] The most widely used probes are fura-2, indo-1, Fluo-3, Calcium Green, and Oregon Green 488 BAPTA-1 (OG1) with *O,O'*-

bis(2-aminophenyl)ethyleneglycol-*N,N,N',N'*-tetraacetic acid (BAPTA) as the Ca^{2+} -selective chelator and benzofuran, benzindole, and fluorescein as the fluorophore.^[3–6] However, the application of these probes with one-photon microscopy (OPM) is limited to use near the tissue surface (< 80 μm).

To observe cellular events deep inside the tissue, it is crucial to use two-photon microscopy (TPM). TPM employing two near-infrared (NIR) photons for excitation offers a number of advantages over OPM, including increased penetration depth (> 500 μm), localized excitation, and prolonged observation time.^[7–9] The extra penetration depth that TPM affords is particularly useful for tissue imaging because surface preparation artifacts, such as damaged cells, extend > 70 μm into the brain slice interior.^[9,10] However, most of the OP fluorescent probes presently used for TPM have small two-photon (TP) action cross sections ($\Phi\delta$) that limit their use in TPM. Another limitation associated with tissue imaging is a mistargeting problem, which results from membrane-bound probes.^[3,11,12] As the probes can be accumulated in any membrane-enclosed structure within the cell, and as the fluorescence quantum yield should be higher in the membrane than in the cytosol, it is practically difficult for the signals from membrane-bound probes to be separated from those of the probe- Ca^{2+} complex. Therefore, there is a need to develop efficient TP probes with 1) enhanced $\Phi\delta$ values for brighter TPM images and 2) larger spectral shifts in different environments for better discrimination between the cytosolic and membrane-bound probes.

[a] H. M. Kim, B. R. Kim, M. J. An, Prof. B. R. Cho
Molecular Opto-Electronics Laboratory
Department of Chemistry
Korea University
1-Anamdong, Seoul 136-701 (Korea)
Fax: (+82)2-3290-3121
E-mail: chobr@korea.ac.kr

[b] Dr. J. H. Hong, Prof. K. J. Lee
National Creative Research Initiative Center for Neurodynamics
and Department of Physics
Korea University
1-Anamdong, Seoul 136-701 (Korea)

 Supporting information for this article contains additional figures and movies of Figures 6 and 7 and is available on the WWW under <http://www.chemeurj.org/> or from the author.

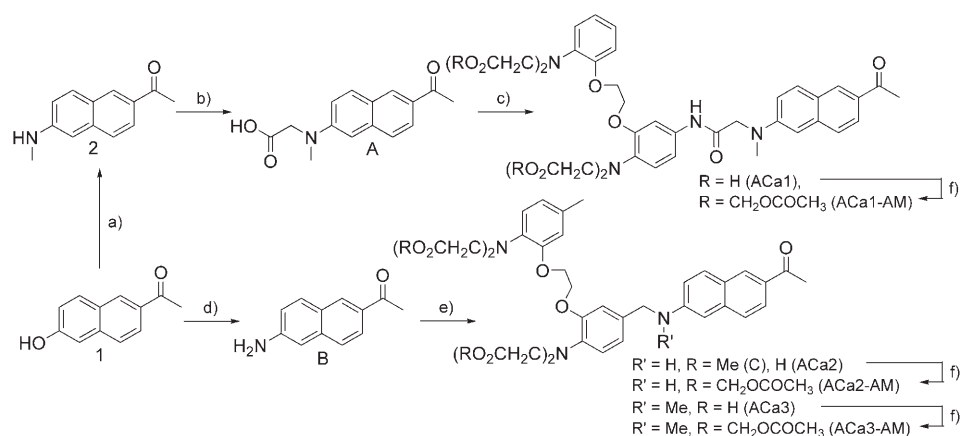
To address these critical needs, we have developed a series of TP probes for Ca^{2+} derived from 2-acetyl-6-(dimethylamino)naphthalene (Acedan) as the TP chromophore and BAPTA as the Ca^{2+} -selective binding site. Acedan is a polarity-sensitive fluorophore that has been successfully employed in the design of TP fluorescent probes for the membrane and metal ions,^[13,14] and BAPTA is the receptor for OG1, a well-known OP fluorescent probe for Ca^{2+} ions.^[3] These findings led us to design Acedan-derived TP fluorescent Ca^{2+} probes (ACa1–ACa3) with the expectation that the probes would emit strong two-photon excited fluorescence (TPEF) on forming complexes with Ca^{2+} . Moreover, if the probe– Ca^{2+} complex emits TPEF in a widely different wavelength range depending on the polarity of the environment, the emission resulting from membrane-bound probes could be excluded from that of the probe– Ca^{2+} complex by using different detection windows. We recently reported an efficient TP probe that can visualize the calcium waves in live tissues.^[14b] Here, we extend our earlier work and present a series of TP fluorescent probes for Ca^{2+} (ACa1–ACa3) that exhibit high selectivity toward Ca^{2+} , emit strong TPEF on forming complexes with Ca^{2+} , and are capable of monitoring the calcium signals in living astrocyte cells and in live mouse tissues at a depth of $>100\ \mu\text{m}$ for a long period of time (1100–4000 s) without photobleaching and mistargeting problems.

Results and Discussion

The synthesis began with the preparation of TP chromophores **A** and **B** (Scheme 1). **A** was prepared by the reaction of **1** with MeNH_2 in the presence of $\text{Na}_2\text{S}_2\text{O}_5$ and NaOH .^[14] Coupling of **A** with 5-amino-BAPTA-tetramethyl ester followed by hydrolysis produced ACa1 in 53% yield. ACa2 was prepared in 74% yield by the reductive amination of **B** with 5-methyl-5'-formyl-BAPTA-tetramethyl ester. Alkylation of ACa2 with methyl iodide afforded ACa3 in 90% yield (Scheme 1). ACa2 and ACa3 were obtained in higher yields and with fewer steps relative to ACa1. To enhance the cell per-

meability, the carboxylic acid moieties were converted to acetoxymethyl esters (ACa1-AM–ACa3-AM).^[15]

The absorption and emission spectra of ACa1 and ACa2 are almost the same (Table 1), probably because the electron-donating effect of the *N*-methyl group is nullified by the electron-withdrawing ability of the amide group between the fluorophore and BAPTA. ACa3 shows a slight bathochromic shift compared to ACa2, indicating an enhanced intramolecular charge transfer (ICT) by the *N*-methyl group. All compounds show gradual bathochromic shifts with the solvent polarity in the order $1,4\text{-dioxane} < \text{DMF} < \text{EtOH} < \text{H}_2\text{O}$ (see Figure S1 and Table S1 in the Supporting Information), and the effects are greater for the emission (72–82 nm) than those for the absorption spectra (17–19 nm). This indicates the potential utility of these compounds as polarity probes. In addition, the $\lambda_{\text{max}}^{\text{fl}}$ values of the AM esters in DMF are similar to those of the membrane-bound



Scheme 1. Synthesis of ACa1–ACa3. a) $\text{MeNH}_2\cdot\text{HCl}$, $\text{Na}_2\text{S}_2\text{O}_5$, NaOH , H_2O ; b) i) $\text{BrCH}_2\text{CO}_2\text{Me}$, Na_2HPO_4 , NaI , MeCN ; ii) KOH , EtOH ; c) i) 5-amino-BAPTA-tetramethyl ester, EDCI , DMAP , DMF ; ii) KOH , EtOH , H_2O ; d) NH_4OH , $\text{Na}_2\text{S}_2\text{O}_5$; e) i) 5-methyl-5'-formyl-BAPTA-tetramethyl ester, $(\text{MeCO}_2)_3\text{BHN}$, DCE ; ii) KOH , EtOH , H_2O (ACa2); iii) C , MeI , proton sponge, MeCN ; iv) KOH , EtOH , H_2O (ACa3); f) $\text{BrCH}_2\text{OCOCH}_3$, Et_3N , CHCl_3 , EDCI : 1-(3-dimethylaminopropyl)-3-ethylcarbodiimide; DMAP : 4-dimethylaminopyridine; DCE : 1,2-dichloroethane.

Table 1. Photophysical data for ACa1–ACa3 and OG1.

| Compound ^[a] | $\lambda_{\text{max}}^{(1)[b]}$ | $\lambda_{\text{max}}^{\text{fl}[c]}$ | $\phi^{\text{fl}[d]}$ | $K_{\text{d}}^{\text{OP}}/K_{\text{d}}^{\text{TP}[e]}$ | FEF/TFEF ^[f] | $\lambda_{\text{max}}^{(2)[g]}$ | $\delta^{\text{fl}[h]}$ | $\phi\delta^{\text{fl}[i]}$ |
|-------------------------|---------------------------------|---------------------------------------|-----------------------|--|-------------------------|---------------------------------|-------------------------|-----------------------------|
| ACa1-AM | 362 | 495 | 0.060 | | | nd ^[j] | nd ^[j] | nd ^[j] |
| ACa1 | 365 | 498 | 0.012 | | | nd ^[j] | nd ^[j] | nd ^[j] |
| ACa1 + Ca^{2+} | 365 | 498 | 0.49 | 0.27 ^[k] /0.25 | 40/44 | 780 | 230 | 110 |
| ACa2-AM | 362 | 494 | 0.014 | | | nd ^[j] | nd ^[j] | nd ^[j] |
| ACa2 | 362 | 495 | 0.010 | | | nd ^[j] | nd ^[j] | nd ^[j] |
| ACa2 + Ca^{2+} | 362 | 495 | 0.42 | 0.14 ^[k] /0.16 nm | 42/50 | 780 | 210 | 90 |
| ACa3-AM | 370 | 499 | 0.032 | | | nd ^[j] | nd ^[j] | nd ^[j] |
| ACa3 | 375 | 500 | 0.015 | | | nd ^[j] | nd ^[j] | nd ^[j] |
| ACa3 + Ca^{2+} | 375 | 517 | 0.38 | 0.13 ^[k] /0.14 nm | 25/23 | 780 | 250 | 95 |
| OG1 + Ca^{2+} | 494 | 523 | 0.66 | 0.17 ^[l] /nd | 14 ^[l] /nd | 800 | 37 | 24 |

[a] All data were measured in 30 mM MOPS, 100 mM KCl, 10 mM EGTA, pH 7.2 in the absence and presence (39 μM) of free Ca^{2+} . [b,c] λ_{max} of the OP absorption and emission spectra, respectively, in nm. [d] Fluorescence quantum yield, $\pm 10\%$. [e] Dissociation constants for Ca^{2+} in μM measured by OP (K_{d}^{OP}) and TP (K_{d}^{TP}) processes, $\pm 14\%$. [f] Fluorescence enhancement factor, $(F - F_{\text{min}})/F_{\text{min}}$, measured by OP (FEF) and TP (TFEF) processes. [g] λ_{max} of the TP excitation spectra in nm. [h] The peak TP cross section in $10^{-50}\ \text{cm}^4\ \text{photon}^{-1}$ (GM), $\pm 15\%$. [i] TP action cross section. [j] nd: not determined; the TPEF intensity was too weak to measure the cross section accurately. [k] K_{d}^{OP} values of ACa1, ACa2, and ACa3 for Mg^{2+} are 6.8 ± 0.7 , 6.2 ± 0.7 , and 6.0 ± 0.6 mM, respectively. [l] Reference [3].

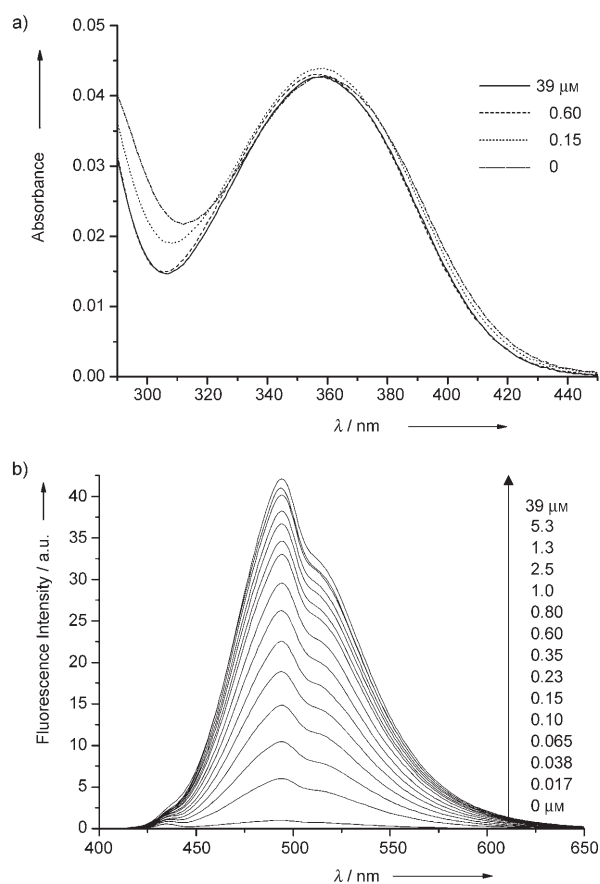


Figure 1. OP absorption (a) and emission (b) spectra of $1 \mu\text{M}$ Aca2 (30 mM MOPS, 100 mM KCl, 10 mM EGTA, pH 7.2) in the presence of free Ca^{2+} (0–39 μM). EGTA: ethylene glycol tetraacetic acid.

probes (Figure 4b and Figure S2 and Table S1 in the Supporting Information), indicating that they could be used as models for the latter (see below).

When Ca^{2+} was added to Aca2 in 3-(*N*-morpholino)propanesulfonic acid (MOPS) buffer solution (30 mM, pH 7.2), the fluorescence intensity increased gradually with the metal-ion concentration without affecting the absorption spectra (Figure 1), probably due to the blocking of the photoinduced electron-transfer (PET) process by the metal-ion complexation.^[16] Similar results were observed for Aca1 and Aca3 in OP and TP processes (Figure 2b, Figures S3 and S4 in the Supporting Information, and reference [14b]). The fluorescence-enhancement factors [FEF = $(F - F_{\text{min}})/F_{\text{min}}$] of Aca1–Aca3 measured by the titration curves were in the range of 23–50 (Table 1). The FEF of Aca2 is nearly identical to that of Aca1, while that of Aca3 is appreciably smaller as a result of the larger fluorescence quantum yield (Φ) in the absence, and smaller Φ in the presence, of excess Ca^{2+} than for the others. All compounds show larger FEFs than the 14 reported for OG1, indicating a greater sensitivity of these probes to the change in the Ca^{2+} -ion concentration.^[3] Moreover, Hill plots for Ca^{2+} binding, measured by OP and TP processes, showed good linear relationships with

a slope of 1.0, indicating 1:1 complexation (Figure 2c and Figure S4b in the Supporting Information).^[17]

The dissociation constants (K_{d}^{OP}) were calculated from the fluorescence titration curves (Figure 2d and Figure S4c in the Supporting Information).^[17,18] The K_{d}^{OP} values of Aca2 and Aca3 for Ca^{2+} were approximately twofold smaller than that of Aca1 (Table 1), indicating higher affinity for Ca^{2+} , which can be attributed to the enhanced electron density at the metal-ion binding sites by the *p*-Me group. Similar values were determined by the TP process (Table 1). This indicates the capabilities of Aca2 and Aca3 to detect lower concentrations of Ca^{2+} than Aca1 by TPM. Moreover, the K_{d}^{OP} values of Aca1–Aca3 for Mg^{2+} are in the range of 6.0–6.8 mM (Table 1 and Figure S6 in the Supporting Information), thus negating the possibility of Mg^{2+} interference.

Aca2 and Aca3 showed a modest response toward Zn^{2+} and Mn^{2+} , a much weaker response toward Mg^{2+} , Fe^{2+} , and Co^{2+} , and no response toward Cu^{2+} (Figure 3a and Figure S5a in the Supporting Information). A similar result was reported for Aca1.^[14b] As the intracellular free-ion concentration of Mn^{2+} is negligible,^[19] these probes can detect the intracellular Ca^{2+} concentration ($[\text{Ca}^{2+}]_{\text{i}}$) in the regions in which the chelatable Zn^{2+} concentration ($[\text{Zn}^{2+}]_{\text{i}}$) is much lower than K_{d}^{TP} (Ca^{2+}). Furthermore, all probes were pH-insensitive in the neutral pH range, although the FEF decreased slightly at pH < 6.5 (Figure 3b, Figure S5b in the Supporting Information, and reference [14b]).

The TP action spectra of the Ca^{2+} complexes with Aca1–Aca3 in buffer solutions indicated the $\Phi\delta$ values of 90–110 GM at 780 nm, approximately fourfold larger than that of OG1– Ca^{2+} (Table 1). Thus, TPM images for samples stained with Aca1–Aca3 would be much brighter than those stained with a commercial probe. In addition, the two-photon fluorescence enhancement factors (TFEFs) estimated from the TP titration curves were in the range of 23–50 (Table 1), values that could allow detection of Ca^{2+} by TPM.

The pseudocolored TPM images of cultured astrocytes labeled with $2 \mu\text{M}$ Aca2-AM showed intense spots and homogeneous domains (Figure 4a). We attributed the image to the TPEF emitted from the intracellular Aca2– Ca^{2+} complex and membrane-bound probes, because the fluorescence quantum yields of Aca2– Ca^{2+} in MOPS buffer (0.42) and Aca2-AM in DMF (0.37) are much higher than those of Aca2 (0.010) and Aca2-AM (0.014) in MOPS buffer (Table 1 and Table S1 in the Supporting Information). In addition, Aca2-AM in DMF has been assumed to be a good model for the membrane-bound probes due to the similarity in $\lambda_{\text{max}}^{\text{fl}}$ (see above). The TPEF spectra of the intense spots and homogeneous domains showed emission maxima at 445 (Figure 4b, blue curve) and 500 nm (red curve), respectively. Moreover, the blue emission band was unsymmetrical and could be fitted to two Gaussian functions with maxima at 440 and 488 nm (sky blue curve), respectively, whereas the red emission band could be fitted to one Gaussian function with maximum at 500 nm (brown curve). Compared with

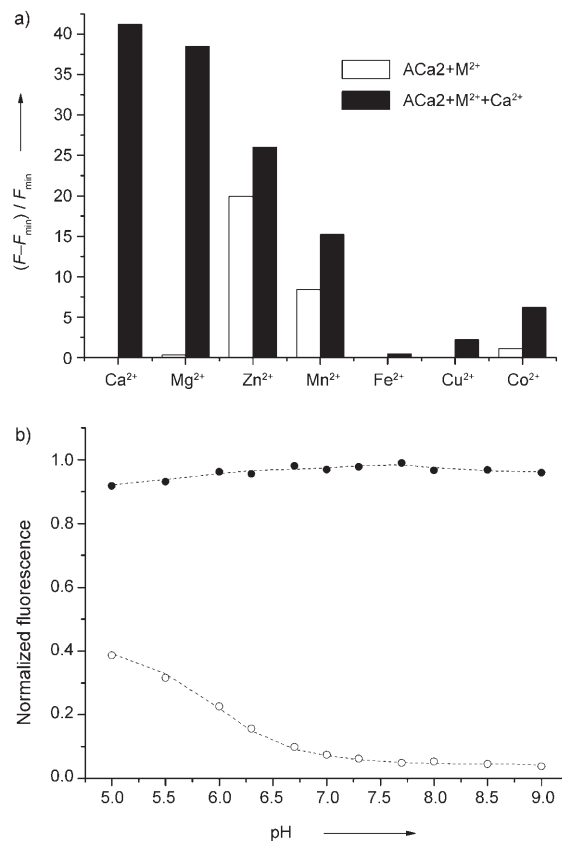
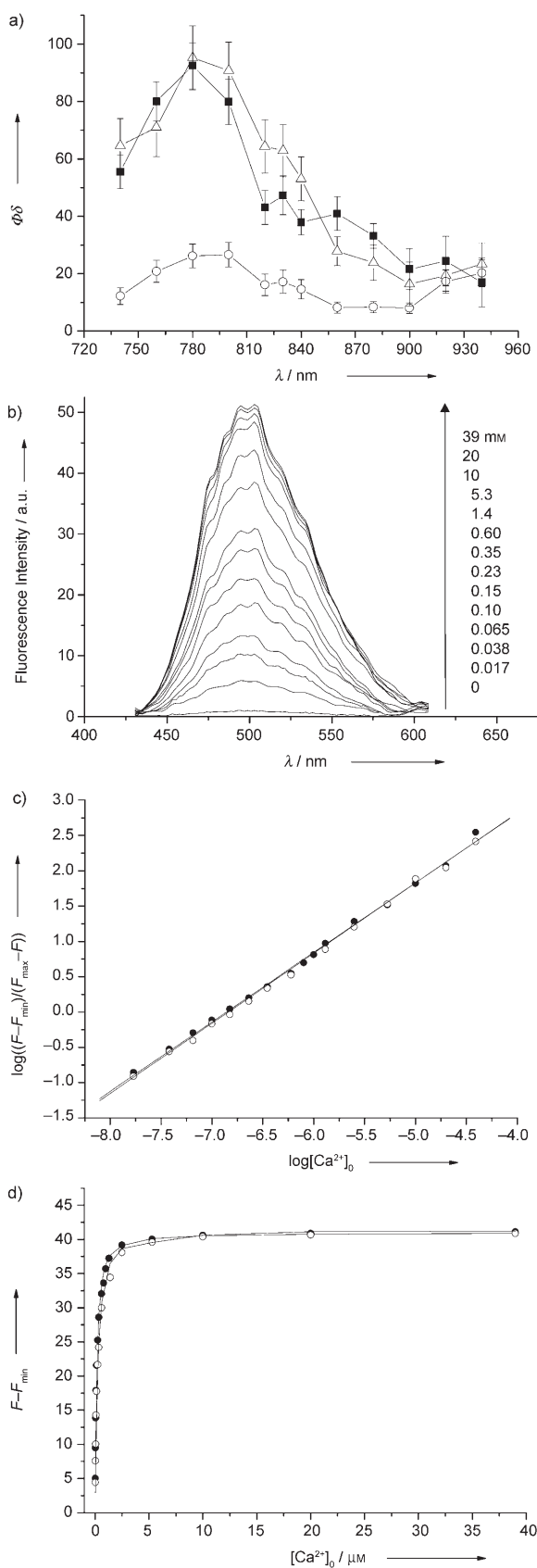


Figure 3. a) Relative fluorescence intensity of 1 μM Aca2 in the presence of 2 mM Mg^{2+} and 100 μM Zn^{2+} , Fe^{2+} , Mn^{2+} , Cu^{2+} , or Co^{2+} (empty bars) followed by addition of 100 μM of Ca^{2+} (filled bars). b) Effect of pH on the OP fluorescence intensity of 1 μM Aca2 in the presence of 0.0 (\circ) and 39 μM (\bullet) of free Ca^{2+} in 30 mM MOPS and 100 mM KCl. The data at $[\text{Ca}^{2+}] = 0 \mu\text{M}$ were determined by adding 10 mM EGTA. These data were measured in 30 mM MOPS buffer (100 mM KCl, 10 mM EGTA, pH 7.2). The excitation wavelength was 365 nm.

the emission spectra recorded in MOPS buffer (Figure 1b), the shorter-wavelength band of the dissected spectrum was significantly blue-shifted, while the longer-wavelength band remained similar (Table 1). The spectral shift suggests that the probes may be located in two regions of differing polarity. Furthermore, the intense spot exhibited an excited-state lifetime of 1.2 ns, which was much longer than the upper extreme of the lifetime distribution curve centered at 0.6 ns (Figure 5). From these results, we hypothesize that the probes are located in two different environments, the more-polar one is cytosol (red emission with a shorter lifetime)

Figure 2. a) TP action spectra of Aca2 (\blacksquare), Aca3 (\triangle), and OG1 (\circ) in the presence of 39 μM free Ca^{2+} . b) TP emission spectra of Aca2 (30 mM MOPS, 100 mM KCl, 10 mM EGTA, pH 7.2) in the presence of free Ca^{2+} (0–39 μM). c) Hill plots for the complexation of Aca2 with free Ca^{2+} (0–39 μM) measured by OP (\bullet) and TP (\circ) processes. d) OP (\bullet) and TP (\circ) fluorescence titration curves for the complexation of Aca2 with various concentrations (0–39 μM) of free Ca^{2+} . The excitation wavelengths for OP and TP processes were 365 and 780 nm, respectively.

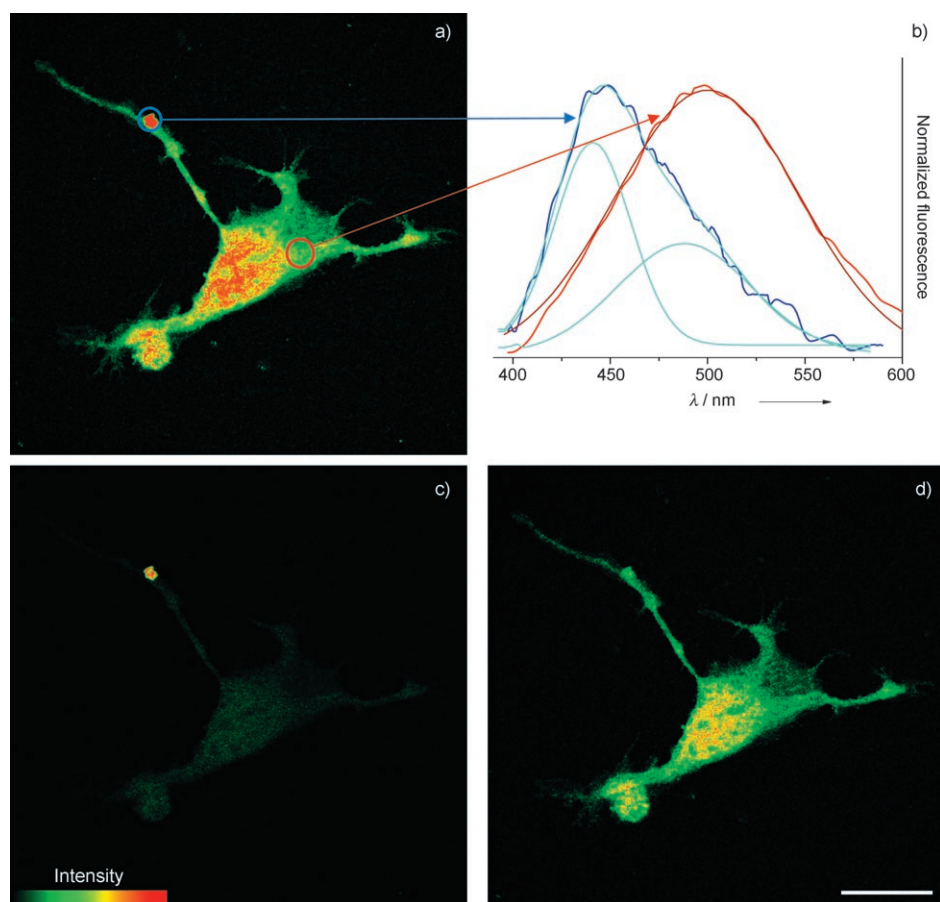


Figure 4. Pseudocolored TPM images of Aca2-AM-labeled ($2\ \mu\text{M}$) astrocytes collected at a) 360–620, c) 360–460, and d) 500–620 nm. b) TPEF spectra from the hydrophobic (blue) and hydrophilic (red) domains of Aca2-AM-labeled astrocytes. The excitation wavelength was 780 nm. Cells shown are representative images from replicate experiments. Scale bar: 30 μm .

and the less-polar one is membrane-associated (blue emission with a longer lifetime).

The intracellular Ca^{2+} could be detected with minimum errors from the membrane-bound probes. The spectrum of the shorter-wavelength band in the dissected Gaussian function (Figure 4b, sky blue curve) decreased to baseline at $\approx 500\ \text{nm}$, indicating that the TPEF emitted from the membrane-bound probes contributes negligible interference at $\lambda > 500\ \text{nm}$. Similarly, if one considers Aca2-AM in DMF as a model for the membrane-bound probe (see above), the fluorescence at $\lambda > 500\ \text{nm}$ accounts for only 5% of the total emission band (Figure S2 in the Supporting Information). Consistently, the TPEF image collected at 500–620 nm is homogeneous without the intense spots (Figure 4d), whereas that collected at 360–460 nm clearly shows them (Figure 4c). Therefore, one can selectively detect the intracellular Ca^{2+} by using the detection window at 500–620 nm.

To demonstrate the utility of this probe, we monitored $[\text{Ca}^{2+}]_i$ waves in live cells and tissue. The TPM images of cultured astrocytes labeled with $2\ \mu\text{M}$ Aca2-AM revealed spontaneous Ca^{2+} signal propagation from the astrocytic process (1) to soma (3) to terminal (5) with a speed of $7.2 \pm$

$2.2\ \text{ms}^{-1}$ ($n=8$ astrocytes; Figure 6a and b, and Movie S1 in the Supporting Information). The spontaneous increase in $[\text{Ca}^{2+}]_i$ was also propagated between astrocytes, as indicated by the delayed activity in the neighboring astrocyte (Figure 6a and c). The speed of propagation of spontaneously occurring waves was $2.1 \pm 1.5\ \text{ms}^{-1}$ ($n=10$ astrocytes). Nearly identical results were reported for Aca1-AM-labeled astrocytes.^[14b] Furthermore, a closer examination of Figure 6a–c reveals that Aca2 can also detect Ca^{2+} in the nucleus. Thus, these probes are clearly capable of visualizing the intra- and intercellular calcium waves in cultured astrocytes by using TPM.

We further investigated the utility of this probe in tissue imaging. Figure 7 reveals the TPM images of individual astrocytes in acute hypothalamic slices from postnatal one-day rat incubated with $10\ \mu\text{M}$ Aca2-AM for 30 min at 37°C . The spontaneous Ca^{2+} waves in the somas (1–3) of neurons and astrocytes could be simultaneously visualized with an average

frequency of about 11 mHz ($n=4$ slices) for more than 4000 s without appreciable decay (Supporting Information, Movie S2). Both the intensity and the frequency of the signals varied significantly depending on the cells. Similarly, Aca1 was capable of detecting the spontaneous Ca^{2+} waves in the hypothalamic slice at a depth of $\approx 170\ \mu\text{m}$ for longer than 1100 s.^[14b] In contrast, OPM images of the tetrodotoxin-treated thalamus slice stained with fura-2^[20] revealed damaged cells on the tissue surface and was not as clear as the TPM image presented here. Also, the fluorescence intensity decayed appreciably after 500 s.^[20] The improved TPM image of Aca2-labeled tissue obtained at a depth of $\approx 120\ \mu\text{m}$ for a prolonged observation time underlines the high photostability and low phototoxicity of this probe, in addition to the capability of deep-tissue imaging. Finally, it has to be mentioned that the use of laser power higher than that of OP fluorescence microscopy ($\approx 10\ \text{mW}$ versus $\approx 20\ \mu\text{W}$) does not in any way cause appreciable damage to the cell and tissue. This can be attributed to the negligible absorption by the sample at 780 nm, which can only lead to vibrational and not the electronic excitation.

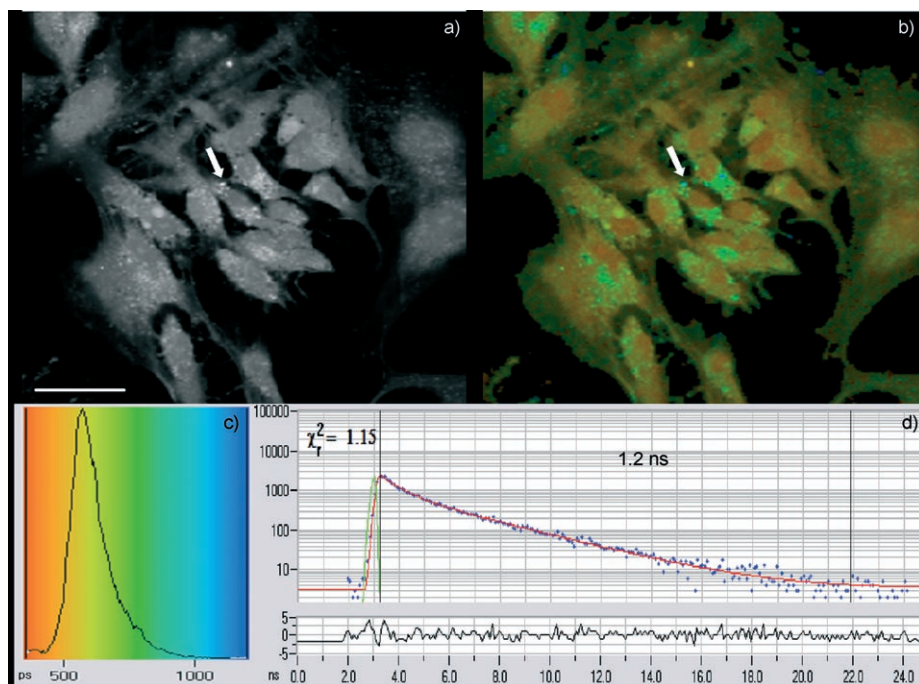


Figure 5. a) OP fluorescence intensity image and b) pseudocolored lifetime image of Aca2-AM-labeled ($2 \mu\text{M}$) astrocytes. The excitation wavelength was 405 nm. c) Lifetime distribution; the average lifetime was ≈ 0.6 ns. d) Single-point analysis of the region indicated by the white arrow gave a lifetime of 1.2 ns. Scale bar: $30 \mu\text{m}$.

Conclusions

We have developed a series of TP probes (ACa1–ACa3) that show 23–50-fold TPEF enhancement in response to Ca^{2+} , dissociation constants (K_d^{TP}) in the range of (0.14 ± 0.02) – $(0.25 \pm 0.03) \mu\text{M}$, and emit fourfold stronger TPEF than OG1 upon complexation with Ca^{2+} . The TP probes can selectively detect dynamic levels of intracellular free Ca^{2+} in live cells and living tissues without interference from other metal ions and membrane-bound probes. Moreover, these probes are capable of monitoring the calcium waves at a depth of 120–170 μm in live tissues for longer than 1100–4000 s by using TPM with no artifacts of photobleaching.

Experimental Section

General methods: Synthetic reagents were purchased from Sigma-Aldrich and TCI, and used without further purification. All solvents were from Riedel-de Haën and Sigma-Aldrich and were distilled prior to use. NMR spectra were obtained on a Varian AS400 MHz spectrophotometer operating at 283 K and both ^1H and ^{13}C NMR spectra were referenced to internal probe standards. IR spectra were obtained by using a Nicolet 380 FTIR instrument, and samples were prepared as KBr pellets. Elemental analyses were performed on a Carlo Erba 1108 element analyzer. Absorption spectra were recorded on a Hewlett-Packard 8453 diode array spectrophotometer, and fluorescence spectra were obtained with Amico-Bowman series 2 luminescence spectrometer with a 1 cm standard quartz cell. The fluorescence quantum yield was determined by using Coumarin 307 as the reference by the literature method.^[21]

Synthesis of ACa1–ACa3: The synthesis of ACa1 has been reported.^[14b] 6-Acyl-2-hydroxynaphthalene^[22] and 5-methyl-5'-formyl-BAPTA-tetramethyl ester^[6a] were prepared by literature methods. The synthesis of other compounds is described below.

6-Acyl-2-naphthylamine (B): A mixture of 6-acyl-2-hydroxynaphthalene (**1**; 5.2 g, 28 mmol), $\text{Na}_2\text{S}_2\text{O}_5$ (13.3 g, 70 mmol), and NH_4OH (150 mL) in a steel-bomb reactor was stirred at 140°C for 96 h. The product was collected by filtration, washed with water, and purified by flash-column chromatography by using hexane/ethyl acetate (1:1) as the eluent. It was further purified by recrystallization from MeOH. Yield: 3.9 g (75%); m.p. 170°C ; ^1H NMR (400 MHz, CDCl_3): $\delta = 8.30$ (d, $J = 1.6$ Hz, 1H), 7.91 (dd, $J = 8.8$, 2.0 Hz, 1H), 7.74 (d, $J = 8.6$ Hz, 1H), 7.58 (d, $J = 9.2$ Hz, 1H), 6.97 (dd, $J = 8.6$, 2.2 Hz, 1H), 6.95 (d, $J = 2.2$ Hz, 1H), 4.05 (brs, 2H), 2.66 ppm (s, 3H); ^{13}C NMR (100 MHz, CDCl_3): $\delta = 198.1$, 147.0, 137.8, 131.6, 131.4, 130.7, 126.7, 126.2, 124.9, 118.9, 108.1, 26.7 ppm; IR (KBr): $\tilde{\nu} = 3436$, 3345, 1662 cm^{-1} ; elemental analysis calcd (%) for $\text{C}_{12}\text{H}_{11}\text{NO}$: C 77.81, H 5.99, N 7.56; found: C 77.78, H 5.86, N 7.59.

Compound C: Sodium triacetoxyborohydride (1.24 g, 5.85 mmol) was added to a mixture of **B** (0.64 g, 3.46 mmol) and 5-methyl-5'-formyl-BAPTA-tetramethyl ester (1.68 g, 2.92 mmol) in dichloroethane (30 mL), and the solution was stirred for 12 h under N_2 . The solvent was removed in vacuo and the product was purified by column chromatography by using chloroform/ethyl acetate/hexane (3:1:1) as the eluent. Yield: 1.6 g (74%); m.p. 86°C ; ^1H NMR (400 MHz, CDCl_3): $\delta = 8.29$ (d, $J = 1.8$ Hz, 1H), 7.91 (dd, $J = 8.8$, 2.0 Hz, 1H), 7.71 (d, $J = 8.6$ Hz, 1H), 7.58 (d, $J = 8.6$ Hz, 1H), 6.92 (m, 3H), 6.73 (m, 5H), 4.51 (brs, 1H), 4.36 (s, 2H), 4.25 (m, 4H), 4.15 (s, 4H), 4.10 (s, 4H), 3.58 (s, 6H), 3.52 (s, 6H), 2.66 (s, 3H), 2.25 ppm (s, 3H); ^{13}C NMR (100 MHz, CDCl_3): $\delta = 198.0$, 172.2, 172.1, 150.8, 150.5, 138.8, 138.1, 136.9, 132.6, 132.4, 131.2, 131.1, 130.6, 126.3, 125.0, 122.0, 120.7, 119.4, 119.1, 118.7, 114.3, 114.2, 112.7, 112.6, 104.8, 67.4, 67.1, 53.6, 53.5, 51.9, 51.7, 47.9, 26.7, 21.2 ppm; IR (KBr): $\tilde{\nu} = 3343$, 1756, 1663 cm^{-1} ; elemental analysis calcd (%) for $\text{C}_{40}\text{H}_{45}\text{N}_5\text{O}_{11}$: C 64.59, H 6.10, N 5.65; found: C 64.49, H 6.15, N 5.54.

ACa2: A mixture of **C** (0.50 g, 0.67 mmol) and KOH (0.30 g, 5.36 mmol) in EtOH/ H_2O (50/10 mL) was stirred for 6 h. The ethanol was evaporated in vacuo, the residue was diluted with ice-water (30 mL), and concentrated HCl aq. was added slowly at $<5^\circ\text{C}$ until pH 3 had been reached. The resulting precipitate was collected and washed with distilled water. Yield: 0.27 g (59%); m.p. 151°C ; ^1H NMR (400 MHz, CD_3OD): $\delta = 8.33$ (d, $J = 1.6$ Hz, 1H), 7.80 (dd, $J = 8.8$, 1.6 Hz, 1H), 7.71 (d, $J = 9.2$ Hz, 1H), 7.50 (d, $J = 8.6$ Hz, 1H), 7.09 (d, $J = 2.0$ Hz, 1H), 7.06 (dd, $J = 9.0$, 2.0 Hz, 1H), 6.94 (dd, $J = 8.8$, 2.0 Hz, 1H), 6.88 (d, $J = 8.8$ Hz, 1H), 6.82 (d, $J = 9.0$ Hz, 1H), 6.77 (d, $J = 1.6$ Hz, 1H), 6.76 (d, $J = 2.0$ Hz, 1H), 6.67 (dd, $J = 9.0$, 2.0 Hz, 1H), 4.37 (s, 2H), 4.32 (t, 2H), 4.26 (t, 2H), 4.02 (s, 4H), 3.96 (s, 4H), 2.62 (s, 3H), 2.42 ppm (s, 3H); ^{13}C NMR (100 MHz, CD_3OD): $\delta = 199.2$, 174.8, 150.7, 149.4, 138.6, 138.0, 136.3, 134.1, 133.1, 130.9, 130.6, 130.1, 126.1, 125.8, 125.7, 124.0, 123.9, 121.5, 120.2, 119.4, 118.8, 118.2, 114.2, 112.7, 67.2, 66.9, 55.2, 55.0, 46.7, 25.3, 25.2, 19.8 ppm; IR (KBr): $\tilde{\nu} = 3350$, 2915, 1750, 1662 cm^{-1} ; elemental analysis calcd (%) for $\text{C}_{36}\text{H}_{37}\text{N}_5\text{O}_{11}$: C 62.87, H 5.42, N 6.11; found: C 62.64, H 5.90, N 6.02.

ACa2-AM: A mixture of ACa2 (0.12 g, 0.17 mmol), bromomethyl acetate (0.21 g, 1.4 mmol), and Et_3N (0.14 g, 1.4 mmol) in CHCl_3 (5 mL) was

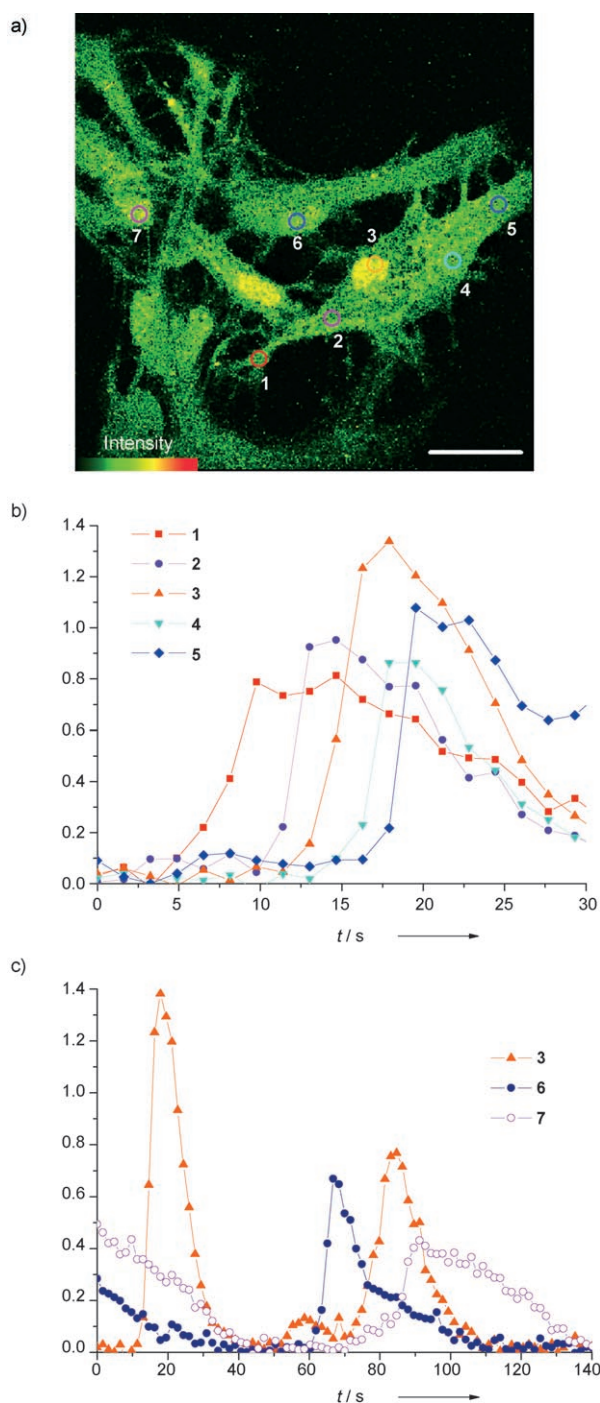


Figure 6. a) Pseudocolored TPM images of ACA2-AM-labeled astrocytes taken after 20 s. b,c) Time courses of the calcium waves in different locations showing the spontaneous intracellular (b) and intercellular (c) Ca²⁺ propagation. All images were collected at 500–620 nm with 1.6 s intervals and the excitation wavelength was 780 nm with femtosecond pulses. Scale bar: 30 μ m.

stirred under N₂ for 24 h. The solvent was removed in vacuo and the crude product was purified by column chromatography by using ethyl acetate/hexane (3:1) as the eluent. It was further purified by recrystallization from MeOH. Yield: 85 mg (51%); m.p. 78 °C; ¹H NMR (400 MHz, CDCl₃): δ = 8.30 (d, J = 1.6 Hz, 1H), 7.91 (dd, J = 8.8, 1.6 Hz, 1H), 7.72 (d, J = 8.6 Hz, 1H), 7.59 (d, J = 9.0 Hz, 1H), 6.95 (m, 3H), 6.75 (m, 5H),

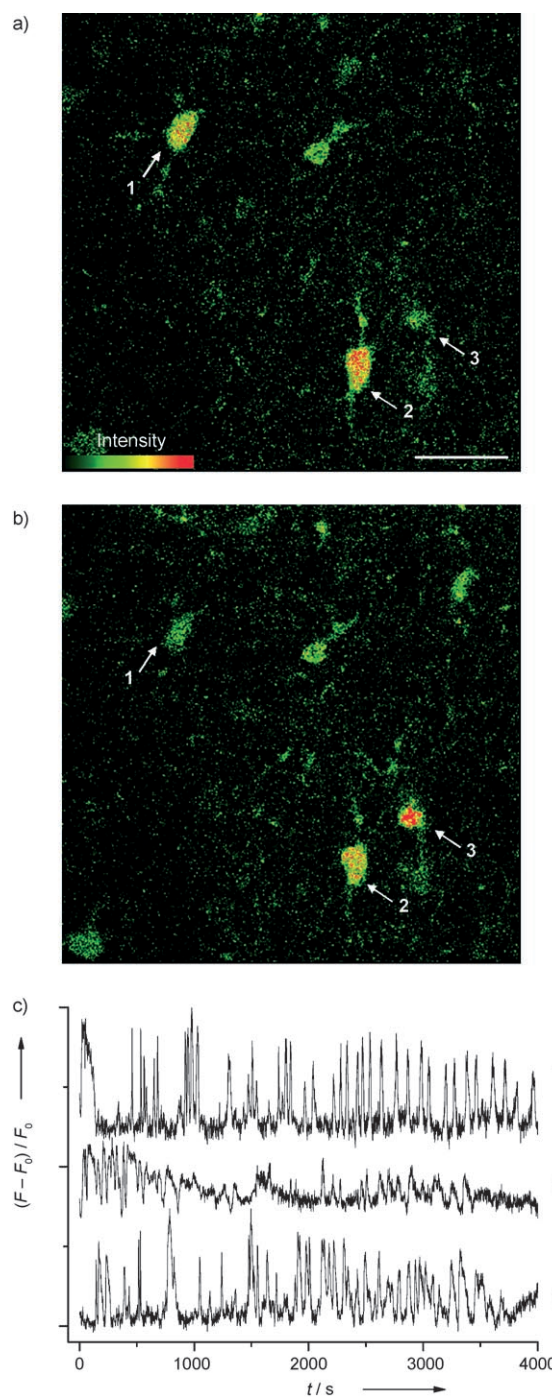


Figure 7. a,b) Pseudocolored TPM images of an acute rat hypothalamic slice stained with 10 μ M ACA2-AM taken after 40 (a) and 1460 s (b). Magnification at 100 \times shows the hypothalamic area at a depth of \approx 120 μ m. c) Spontaneous Ca²⁺ transients recorded in cells (1–3). The TPEF images were collected at 500–620 nm with 1.6 s intervals and the excitation wavelength was 780 nm with femtosecond pulses. Scale bar: 30 μ m.

5.61 (s, 4H), 5.56 (s, 4H), 4.65 (brs, 1H), 4.36 (s, 2H), 4.27 (s, 4H), 4.20 (s, 4H), 4.15 (s, 4H), 2.67 (s, 3H), 2.27 (s, 3H), 2.07 (s, 6H), 2.05 ppm (s, 6H); ¹³C NMR (100 MHz, CDCl₃): δ = 198.1, 170.5, 170.4, 169.8, 169.7, 150.9, 150.6, 148.4, 138.2, 136.3, 135.4, 133.4, 133.1, 131.2, 131.1, 130.6, 130.4, 126.3, 125.0, 122.2, 121.1, 119.8, 118.8, 114.5, 114.4, 113.0, 104.0, 79.5, 79.4, 79.3, 67.4, 67.1, 53.6, 53.5, 47.9, 26.7, 22.9, 20.9 ppm; IR (KBr):

$\bar{\nu} = 3345, 1750, 1710, 1662 \text{ cm}^{-1}$; elemental analysis calcd (%) for $\text{C}_{48}\text{H}_{53}\text{N}_5\text{O}_{19}$: C 59.07, H 5.47, N 4.31; found: C 58.80, H 5.78, N 4.12.

ACa3: Compound **C** (0.80 g, 1.08 mmol) was dissolved in MeCN (30 mL) and proton sponge (0.46 g, 2.15 mmol), NaI (0.032 g, 0.22 mmol), and CH_3I (0.46 g, 3.24 mmol) were added. The reaction mixture was refluxed for 12 h under N_2 . The solvent was removed in vacuo and the product was purified by column chromatography by using chloroform/ethyl acetate/hexane (3:1:1) as the eluent. Yield: 0.73 g (90%); m.p. 82 °C; $^1\text{H NMR}$ (400 MHz, CDCl_3): $\delta = 8.30$ (d, $J = 1.6$ Hz, 1H), 7.91 (dd, $J = 8.6, 1.8$ Hz, 1H), 7.76 (d, $J = 8.8$ Hz, 1H), 7.60 (d, $J = 9.0$ Hz, 1H), 7.16 (dd, $J = 9.0, 2.0$ Hz, 1H), 6.90 (d, $J = 2.0$ Hz, 1H), 6.66 (m, 6H), 4.60 (s, 2H), 4.20 (s, 4H), 4.13 (s, 4H), 4.08 (s, 4H), 3.55 (s, 6H), 3.51 (s, 6H), 3.14 (s, 3H), 2.67 (s, 3H), 2.25 ppm (s, 3H); $^{13}\text{C NMR}$ (100 MHz, CDCl_3): $\delta = 198.0, 172.3, 172.2, 150.8, 150.4, 138.5, 137.9, 136.9, 132.4, 132.2, 131.0, 130.6, 126.4, 125.4, 124.8, 121.9, 119.7, 119.3, 119.1, 116.6, 114.2, 111.4, 105.6, 67.2, 67.0, 58.7, 56.3, 53.6, 53.5, 51.8, 51.7, 39.0, 26.7, 21.2, 18.7$ ppm; IR (KBr): $\bar{\nu} = 1756, 1662 \text{ cm}^{-1}$; elemental analysis calcd (%) for $\text{C}_{41}\text{H}_{47}\text{N}_5\text{O}_{11}$: C 64.98, H 6.25, N 5.54; found: C 65.04, H 6.19, N 5.59.

This ester (0.50 g, 0.66 mmol) was hydrolyzed by the method described above. Yield: 0.24 g (52%); m.p. 141 °C; $^1\text{H NMR}$ (400 MHz, CD_3OD): $\delta = 8.35$ (d, $J = 1.8$ Hz, 1H), 7.82 (dd, $J = 8.8, 1.6$ Hz, 1H), 7.79 (d, $J = 8.8$ Hz, 1H), 7.59 (d, $J = 9.0$ Hz, 1H), 7.26 (dd, $J = 9.0, 2.0$ Hz, 1H), 6.98 (d, $J = 2.0$ Hz, 1H), 6.82 (m, 6H), 4.67 (s, 2H), 4.25 (m, 4H), 3.96 (s, 4H), 3.90 (s, 4H), 3.16 (s, 3H), 2.63 (s, 3H), 2.24 ppm (s, 3H); $^{13}\text{C NMR}$ (100 MHz, CD_3OD): $\delta = 199.0, 172.6, 172.5, 150.4, 150.2, 138.4, 138.1, 137.6, 135.3, 134.2, 130.8, 130.7, 125.1, 124.7, 121.3, 119.4, 119.1, 118.7, 118.4, 116.2, 114.3, 112.7, 112.1, 105.8, 67.3, 67.0, 58.3, 56.3, 54.5, 51.6, 39.2, 25.3, 19.0$ ppm; IR (KBr): $\bar{\nu} = 2915, 1748, 1663 \text{ cm}^{-1}$; elemental analysis calcd (%) for $\text{C}_{37}\text{H}_{39}\text{N}_5\text{O}_{11}$: C 63.33, H 5.60, N 5.99; found: C 63.22, H 5.75, N 5.91.

ACa3-AM: This compound was prepared by using the procedure described for ACa2-AM. Yield: 54%; m.p. 102 °C; $^1\text{H NMR}$ (400 MHz, CDCl_3): $\delta = 8.30$ (d, $J = 1.6$ Hz, 1H), 7.92 (dd, $J = 8.6, 1.6$ Hz, 1H), 7.77 (d, $J = 8.8$ Hz, 1H), 7.62 (d, $J = 9.0$ Hz, 1H), 7.17 (dd, $J = 9.0, 2.0$ Hz, 1H), 6.93 (d, $J = 2.0$ Hz, 1H), 6.74 (m, 6H), 5.60 (s, 4H), 5.58 (s, 4H), 4.60 (s, 2H), 4.22 (s, 4H), 4.17 (s, 4H), 4.14 (s, 4H), 3.15 (s, 3H), 2.67 (s, 3H), 2.26 (s, 3H), 2.05 (s, 6H), 2.04 ppm (s, 6H); $\delta = 198.0, 171.1, 170.8, 169.7, 169.6, 150.5, 150.2, 148.7, 138.6, 136.3, 135.4, 133.3, 133.2, 131.7, 131.6, 130.8, 130.5, 126.5, 125.2, 122.7, 121.1, 119.8, 118.8, 114.7, 114.6, 113.2, 104.0, 79.7, 79.5, 79.4, 68.4, 68.1, 54.6, 54.5, 47.9, 42.8, 26.7, 23.2, 21.0$ ppm; IR (KBr): $\bar{\nu} = 1750, 1710, 1660 \text{ cm}^{-1}$; elemental analysis calcd (%) for $\text{C}_{49}\text{H}_{55}\text{N}_5\text{O}_{19}$: C 59.45, H 5.60, N 4.24; found: C 59.42, H 5.54, N 4.30.

Determination of apparent dissociation constants: A series of calibration solutions containing various $[\text{Ca}^{2+}]$ was prepared by mixing two solutions (solution A, containing 10 mM K_2EGTA , and solution B, containing 10 mM CaEGTA) in various ratios.^[3,23] Both solutions contained ACa1–ACa3 (1 μM), KCl (100 mM), and MOPS (30 mM), and were adjusted to pH 7.2.

To determine the K_d values for Ca^{2+} complexes with ACa1–ACa3, the fluorescence spectrum was recorded with solution A (2.0 mL; 0 μM free Ca^{2+}) at 20 °C. Then this solution (203 μL) was discarded and replaced by solution B (203 μL ; 39 μM free Ca^{2+}), and the spectrum was recorded. This brought the CaEGTA concentration to 1.00 mM and $[\text{Ca}^{2+}]_{\text{free}}$ to about 0.017 μM with no change in the concentration of the probe or of the total EGTA. $[\text{Ca}^{2+}]_{\text{free}}$ was calculated from the K_d of EGTA for Ca^{2+} (150.5 nM) by using Equation (1).^[3,23]

$$[\text{Ca}^{2+}]_{\text{free}} = K_d^{\text{EGTA}} \times \frac{[\text{CaEGTA}]}{[\text{K}_2\text{EGTA}]} \quad (1)$$

Further iterations attained 0.038, 0.065, 0.101, 0.150, 0.230, 0.350, 0.601, 0.800, 1.00, 1.30, 2.50, 5.30, 10.0, and 20.0 μM free Ca^{2+} by successively discarding 223, 251, 285, 327, 421, 479, 667, 420, 350, 412, 905, 1028, 926, and 992 μL of solution A and replacing each with an equal volume of solution B.

When a 1:1 metal–ligand complex is formed between probe and Ca^{2+} , one can describe the equilibrium as follows, in which L and M represent

probe and Ca^{2+} , respectively. The total probe and metal-ion concentrations are defined as $[\text{L}]_0 = [\text{L}] + [\text{LM}]$ and $[\text{M}]_0 = [\text{M}] + [\text{LM}]$, respectively. With $[\text{L}]_0$ and $[\text{M}]_0$, the value of K_d is given by [Eq. (2)]:

$$[\text{LM}]^2 - ([\text{L}]_0 + [\text{M}]_0 + K_d)[\text{LM}] + [\text{L}]_0[\text{M}]_0 = 0, [\text{LM}] = \frac{([\text{L}]_0 + [\text{M}]_0 + K_d) - \sqrt{([\text{L}]_0 + [\text{M}]_0 + K_d)^2 - 4[\text{L}]_0[\text{M}]_0}}{2} \quad (2)$$

or [Eq. (3)]:

$$(F - F_{\text{min}}) = \left(\frac{([\text{L}]_0 + [\text{M}]_0 + K_d) - \sqrt{([\text{L}]_0 + [\text{M}]_0 + K_d)^2 - 4[\text{L}]_0[\text{M}]_0}}{2[\text{L}]_0} \right) (F_{\text{max}} - F_{\text{min}}) \quad (3)$$

in which F is the observed fluorescence intensity, F_{min} is the minimum fluorescence intensity, and F_{max} is the maximum fluorescence intensity. The K_d value that best fits the titration curve (Figure 2d and Figure S3c in the Supporting Information) with Equation (3) was calculated by using the Excel program as reported.^[18]

To determine K_d^{TP} for the TP process, the TPEF spectra were obtained with a DM IRE2 microscope (Leica) by using the $x\gamma\lambda$ mode at a scan speed of 800 Hz. They were excited by a mode-locked titanium–sapphire laser source (Coherent Chameleon, 90 MHz, 200 fs) set at a wavelength of 780 nm and output power 1180 mW, which corresponded to approximately 10 mW average power in the focal plane. The TPEF titration curves (Figure 2d and Figure S3c in the Supporting Information) were obtained and fitted to Equation (3).

Measurement of a two-photon cross-section: The TP cross-section (δ) was determined by using the femtosecond fluorescence measurement technique as described previously.^[24] ACa1–ACa3 and OG1 were dissolved in MOPS buffer (30 mM; 100 mM KCl, 10 mM EGTA, pH 7.2) at concentrations of 1.0×10^{-5} M and then the TP-induced fluorescence intensity was measured at 740–940 nm by using fluorescein (8.0×10^{-5} M, pH 11) as the reference, the TP property of which has been well characterized in the literature.^[25] The intensities of the TP-induced fluorescence spectra of the reference and sample emitted at the same excitation wavelength were determined. The TPA cross-section was calculated according to Equation (4):

$$\delta = \frac{S_{\text{r}} \Phi_{\text{r}} \phi_{\text{r}} c_{\text{r}}}{S_{\text{s}} \Phi_{\text{s}} \phi_{\text{s}} c_{\text{s}}} \delta_{\text{r}} \quad (4)$$

Cell culture: Astrocytes were taken from cerebral cortices of one-day-old rats (Sprague–Dawley; SD). Cerebral cortices were dissociated in Hank's balanced salt solution (Gibco BRL, Gaithersburg, MD, USA), containing papain (3 U mL^{-1} ; Worthington Biochemical Corporation, NJ, USA) and plated in 75 mm flasks. To prepare a purified astrocyte culture, the flasks were shaken for 6 h on a shaker at 37 °C and the floating cells that were displaced into the medium were removed. Astrocytes were passaged with 5 min exposure to 0.25% trypsin, replated onto poly(D-lysine)-coated glass coverslips at 50–100 cells per mm^2 , and maintained in Dulbecco's modified Eagle's medium (DMEM; Gibco) supplemented with penicillin/streptomycin and 10% fetal bovine serum (FBS; Gibco) in a CO_2 incubator at 37 °C. After 7–15 days in vitro, the astrocytes were washed three times with serum-free medium, and then incubated with ACa2-AM (2 μM) in serum-free medium for 20 min at 37 °C. The cells were washed three times with phosphate-buffered saline (PBS; Gibco) and then imaged after further incubation in colorless serum-free medium for 15 min.

Two-photon fluorescence microscopy: TP fluorescence microscopy images of ACa2-AM-labeled astrocytes and tissues were obtained with spectral confocal and multiphoton microscopes (Leica TCS SP2) with a $\times 100$ oil objective and numerical aperture (NA) = 1.30. The images were obtained with a DM IRE2 microscope (Leica) by exciting the probes with a mode-locked titanium–sapphire laser source (Coherent Chameleon, 90 MHz, 200 fs) set at a wavelength of 780 nm and output power 1180 mW, which corresponded to approximately 10 mW average power in

the focal plane. To obtain images in the ranges 360–620, 360–460, and 500–620 nm, internal photomultiplier tubes were used to collect the signals in 8-bit unsigned 512 × 512 pixels at a scan speed of 400 Hz.

Fluorescence lifetime imaging microscopy (FLIM): Astrocytes were grown on coverslips in 10% FBS that contained DMEM. The cells were washed briefly in PBS and incubated with Aca2-AM (2 μM) for 20 min at 37°C. The cells were washed with PBS three times, fixed with formaldehyde (3.7% in PBS) for 10 min, washed with PBS three times, and then mounted with mounting solution. The fluorescence decays were resolved by time-correlated single-photon counting by using an SPC830 acquisition board (Becker & Hickl, Berlin) synchronized with a Leica TSC-SP2-AOBS confocal microscope.

Preparation and staining of acute rat hippocampal and hypothalamic slices: Slices were prepared from the hippocampi and the hypothalami of two-day-old rats (SD). Coronal slices were cut into 400-μm-thick slices by using a vibrating-blade microtome in artificial cerebrospinal fluid (ACSF; 138.6 mM NaCl, 3.5 mM KCl, 21 mM NaHCO₃, 0.6 mM NaH₂PO₄, 9.9 mM D-glucose, 1 mM CaCl₂, and 3 mM MgCl₂). Slices were incubated with Aca2-AM (10 μM) in ACSF bubbled with 95% O₂ and 5% CO₂ for 30 min at 37°C. The slices were then washed three times with ACSF, transferred to glass-bottomed dishes (MatTek), and observed in a spectral confocal multiphoton microscope.

Acknowledgements

This work was supported by a Korea Science and Engineering Foundation (KOSEF) grant funded by the Korean government (MOST) (no. R0A-2007-000-20027-0).

- [1] a) M. D. Bootman, M. J. Berridge, *Cell* **1995**, *83*, 675–678; b) M. D. Bootman, M. J. Berridge, P. Lipp, *Cell* **1997**, *91*, 367–373; c) M. D. Bootman, M. J. Berridge, P. Lipp, *Nature* **1998**, *395*, 645–648; d) D. E. Clapham, *Cell* **1995**, *80*, 259–268.
- [2] a) M. J. Berridge, P. Lipp, M. D. Bootman, *Nat. Rev. Mol. Cell Biol.* **2000**, *1*, 11–21; b) M. J. Berridge, M. D. Bootman, H. L. Roderick, *Nat. Rev. Mol. Cell Biol.* **2003**, *4*, 517–529; c) S. Orrenius, B. Zhivotovskiy, P. Nicotera, *Nat. Rev. Mol. Cell Biol.* **2003**, *4*, 552–565; d) R. Rizzuto, T. Pozzan, *Physiol. Rev.* **2006**, *86*, 369–408.
- [3] *The Handbooks—A Guide to Fluorescent Probes and Labeling Technologies*, 10th ed. (Ed.: R. P. Haugland), Molecular Probes, Eugene, **2005**.
- [4] R. Rudolf, M. Mongillo, R. Rizzuto, T. Pozzan, *Nat. Rev. Mol. Cell Biol.* **2003**, *4*, 579–586.
- [5] R. Y. Tsien, *Biochemistry* **1980**, *19*, 2396–2404.
- [6] a) G. Grynkiewicz, M. Poenie, R. Y. Tsien, *J. Biol. Chem.* **1985**, *260*, 3440–3450; b) A. Minta, J. P. Kao, R. Y. Tsien, *J. Biol. Chem.* **1989**, *264*, 8171–8178.
- [7] a) W. Denk, J. H. Strickler, W. W. Webb, *Science* **1990**, *248*, 73–76; b) P. T. C. So, C. Y. Dong, B. R. Masters, K. M. Berland, *Annu. Rev. Biomed. Eng.* **2000**, *2*, 399–429; c) F. Helmchen, W. Denk, *Curr. Opin. Neurobiol.* **2002**, *12*, 593–601.
- [8] a) M. D. Cahalan, I. Parker, S. H. Wei, M. J. Miller, *Nat. Rev. Immunol.* **2002**, *2*, 872–880; b) W. R. Zipfel, R. M. Williams, W. W. Webb, *Nat. Biotechnol.* **2003**, *21*, 1369–1377; c) F. Helmchen, W. Denk, *Nat. Methods* **2005**, *2*, 932–940.
- [9] R. M. Williams, W. R. Zipfel, W. W. Webb, *Curr. Opin. Chem. Biol.* **2001**, *5*, 603–608.
- [10] K. Svoboda, R. Yasuda, *Neuron* **2006**, *50*, 823–839.
- [11] a) C. L. Slayman, V. V. Mousattos, W. W. Webb, *J. Exp. Biol.* **1994**, *196*, 419–438; b) M. J. Petr, R. D. Wurster, *Cell Calcium* **1997**, *21*, 233–240.
- [12] D. Thomas, S. C. Tovey, T. J. Collins, M. D. Bootman, M. J. Berridge, P. Lipp, *Cell Calcium* **2000**, *28*, 213–223.
- [13] H. M. Kim, H.-J. Choo, S.-Y. Jung, Y.-G. Ko, W.-H. Park, S.-J. Jeon, C. H. Kim, T. Joo, B. R. Cho, *ChemBioChem* **2007**, *8*, 553–559.
- [14] a) H. M. Kim, C. Jung, B. R. Kim, S.-Y. Jung, J. H. Hong, Y.-G. Ko, K. J. Lee, B. R. Cho, *Angew. Chem.* **2007**, *119*, 3530–3533; *Angew. Chem. Int. Ed.* **2007**, *46*, 3460–3463; b) H. M. Kim, B. R. Kim, J. H. Hong, J.-S. Park, K. J. Lee, B. R. Cho, *Angew. Chem.* **2007**, *119*, 7589–7592; *Angew. Chem. Int. Ed.* **2007**, *46*, 7445–7448; *Angew. Chem. Int. Ed.* **2007**, *46*, 7445–7448.
- [15] R. Y. Tsien, *Nature* **1981**, *290*, 527–528.
- [16] a) A. P. de Silva, H. Q. N. Gunaratne, T. Gunnlaugsson, A. J. M. Huxley, C. P. McCoy, J. T. Rademacher, T. E. Rice, *Chem. Rev.* **1997**, *97*, 1515–1566; b) B. Valeur, I. Leray, *Coord. Chem. Rev.* **2000**, *205*, 3–40.
- [17] K. A. Connors, *Binding Constants*, Wiley, New York, **1987**.
- [18] a) J. R. Long, R. S. Drago, *J. Chem. Educ.* **1982**, *59*, 1037–1039; b) K. Hirose, *J. Inclusion Phenom. Macrocyclic Chem.* **2001**, *39*, 193–209.
- [19] L. A. Finney, T. V. O'Halloran, *Science* **2003**, *300*, 931–936.
- [20] H. R. Parri, T. M. Gould, V. Crunelli, *Nat. Neurosci.* **2001**, *4*, 803–812.
- [21] J. N. Demas, G. A. Crosby, *J. Phys. Chem.* **1971**, *75*, 991–1024.
- [22] J.-R. Li, G. Zhang, *J. Chem. Crystallogr.* **2005**, *35*, 789–793.
- [23] a) R. Y. Tsien, T. Pozzan, T. J. Rink, *J. Cell Biol.* **1982**, *94*, 325–334; b) R. Y. Tsien, T. Pozzan, *Methods Enzymol.* **1989**, *172*, 230–261; c) A. Takahashi, P. Camacho, J. D. Lechleiter, B. Herman, *Physiol. Rev.* **1999**, *79*, 1089–1125.
- [24] S. K. Lee, W. J. Yang, J. J. Choi, C. H. Kim, S.-J. Jeon, B. R. Cho, *Org. Lett.* **2005**, *7*, 323–326.
- [25] C. Xu, W. W. Webb, *J. Opt. Soc. Am. B* **1996**, *13*, 481–491.

Received: September 13, 2007
Published online: January 3, 2008